

## Supporting Information

### **Multi-interfaces MoS<sub>2</sub>/Ni<sub>3</sub>S<sub>4</sub>/Mo<sub>2</sub>S<sub>3</sub> composite as efficient electrocatalyst for hydrogen evolution reaction in a wide pH range**

Rui Sun,<sup>a</sup> Zhifeng Zhao,<sup>\*b</sup> Zhanhua Su,<sup>b</sup> Tiansheng Li,<sup>a</sup> Jingxiang Zhao,<sup>\*a</sup> and Yongchen Shang<sup>\*a</sup>

<sup>a</sup>*College of Chemistry and Chemical Engineering, Harbin Normal University, Harbin, 150025,*

*China*

<sup>b</sup>*College of Chemistry, Guangdong University of Petrochemical Technology, Maoming, 525000,*

*China*

## I. Experimental Section

### 1. Materials and Characterizations

All reagents are commercially available and used as received without further purification. Pattern X-ray diffraction (PXRD) was recorded using a Bruke D8 equipped with Cu-K $\alpha$  radiation. X-ray photon-electron Spectroscopy (XPS) analysis was performed using a VG ESCALAB MK II spectrophotometer with Mg-K $\alpha$  radiation (1253.6 eV). Scanning electron microscopy (SEM) test was carried out on a Hitachi S-4800 instrument at an accelerating voltage of 5 kV. The transmission electron microscopy (TEM) and high resolution TEM (HRTEM) was performed on a JEM-F200 electron microscope (JEOL, Japan) with an acceleration voltage of 200 kV.

### 2. Synthesis of $(\text{NH}_4)_4[\text{NiH}_6\text{Mo}_6\text{O}_{24}] \cdot 5\text{H}_2\text{O}$

The  $(\text{NH}_4)_4[\text{NiH}_6\text{Mo}_6\text{O}_{24}] \cdot 5\text{H}_2\text{O}$  (abbreviated to NiMo<sub>6</sub>) was prepared according to a modified published procedure.<sup>1</sup>  $(\text{NH}_4)_6\text{Mo}_7\text{O}_{24} \cdot 4\text{H}_2\text{O}$  (5.2073 g, 4.2135 mmol) was dissolved in water (80 mL) and then heated to 100°C.  $\text{Ni}(\text{NO}_3)_2 \cdot 6\text{H}_2\text{O}$  (0.6717 g, 2.3099 mmol) was dissolved in water (20 mL), which was added to the above solution with stirring. The mixture was kept heating and stirring to give rise to a blue solution. The crude product was isolated with evaporation and filtration. The light blue targeted product was obtained by recrystallization in hot water (80 °C) two times, then dried under vacuum. The purity of NiMo<sub>6</sub> was confirmed with the PXRD. As shown in Fig.S1, the peaks at 8.0°, 11.0°, 12.3°, 15.3°, 16.4°, 17.4°, 23.8°, 28.5°, 29.5°, 32.1°, 33.0° and 34.1°, can be clearly observed, which are assigned to the characteristic peaks of  $(\text{NH}_4)_4[\text{NiH}_6\text{Mo}_6\text{O}_{24}] \cdot 5\text{H}_2\text{O}$  (PDF# 22-0506).

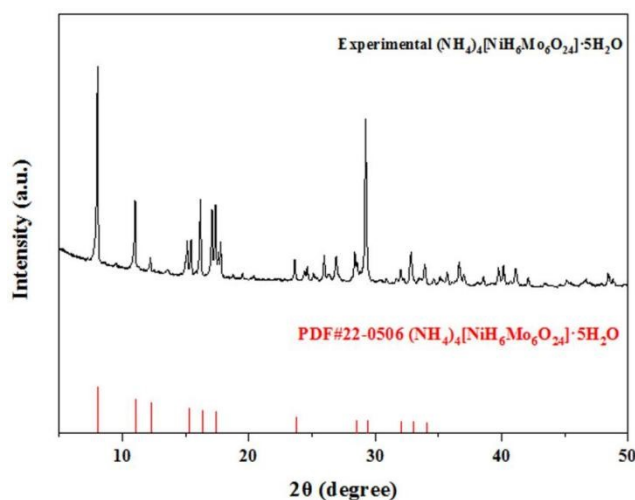


**Fig.S1** PXRD patterns of NiMo<sub>6</sub>.

### 3. Synthesis of the MoS<sub>2</sub>/Ni<sub>3</sub>S<sub>4</sub>/Mo<sub>2</sub>S<sub>3</sub>/CC-xh (x= 20,24, 28 and 32)

Carbon cloth (CC) was initially pretreated by ethanol, acetone and water ultrasonic for 30 min, respectively, and then transferred into Teflon-lined stainless steel reactor and heated at 100 °C for 2 h in concentrated nitric acid, removing the residual organic species before the experiment.

First, NiMo<sub>6</sub> (0.2616 g, 0.2205 mmol), thiourea (TU) (0.3206 g, 4.2118 mmol) and Ni(NO<sub>3</sub>)<sub>2</sub>·6H<sub>2</sub>O (0.0694 g, 0.2387 mmol) were dissolved in 15 mL water, and then one piece of CC (geometric surface area, 1 × 1.5 cm<sup>2</sup>) was put into solution, and sonication for 60 min to form suspension. The suspension was transferred into a 25mL Teflon-lined stainless steel reactor at 200°C for 20h, 24h, 28h and 32h, respectively, then achieving MoS<sub>2</sub>/Ni<sub>3</sub>S<sub>4</sub>/Mo<sub>2</sub>S<sub>3</sub>/CC-xh (where x is hydrothermal reaction time, x= 20, 24, 28 and 32) , samples were washed by distilled water for several time, followed by drying at 60°C overnight.

As a contrast, the electrode containing 1 mg cm<sup>-2</sup> Pt/C on CC was prepared as the following: 5 mg of 20% Pt/C powder was dispersed in 1 mL of solution containing 0.95 mL of ethanol and 50 μL of 0.5 wt% Nafion. Then the mixture was ultrasonicated for 30 min to generate a homogeneous slurry. Finally, an appropriate amount of Pt/C slurry was daubed uniformly over 1 cm<sup>2</sup> of area on a piece of 1 cm × 2 cm CC and dried at room temperature for 24 h.

### 4. Synthesis of the MoS<sub>2</sub>/Ni<sub>3</sub>S<sub>4</sub>/CC

NiMo<sub>6</sub> (0.2616 g, 0.2205 mmol) and thiourea (TU) (0.3206 g, 4.2118 mmol) were dissolved in 15 mL water, and then one piece of CC (geometric surface area, 1 × 1.5 cm<sup>2</sup>) was put into solution, and sonication for 60 min to form suspension. The suspension was transferred into a 25mL Teflon-lined stainless steel reactor at 200°C for 24h, then achieving samples, which were washed by distilled water for several time, followed by drying at 60°C overnight.

## 5. Electrochemical measurements

Both cyclic voltammetry (CV), linear sweep voltammetry (LSV) tests, current density vs time (I-t) curves, electrochemically active surface area (ECSA) and Electrochemical Impedance Spectroscopy (EIS) were conducted with a CHI760E workstation in a conventional three electrode system. MoS<sub>2</sub>/Ni<sub>3</sub>S<sub>4</sub>/Mo<sub>2</sub>S<sub>3</sub>/CC-xh series electrodes (S = 1 cm<sup>2</sup>) served as the working electrode in electrochemical experiments, and a using Ag/AgCl electrode as the reference electrode. And, graphite rod was considered as counter electrode. All the final potentials were expressed in reference to the reversible hydrogen electrode (RHE) via the Nernst equation: in 0.5 M H<sub>2</sub>SO<sub>4</sub>,  $E_{\text{RHE}} = E_{\text{Ag/AgCl}} + 0.059\text{pH} + 0.197$ . where pH is the pH value of the electrolyte solution. For 0.5 M H<sub>2</sub>SO<sub>4</sub> solution, the pH value is 0.3. For 1 M KOH solution, the pH value is 14. Linear sweep voltammetry (LSV) was measured to study the HER performance at the rate of 5 mV s<sup>-1</sup>. The Tafel data were fitted according to the equation  $\eta = b \log(j) + \alpha$  (j: current density, and b:Tafel slope). The durability tests were carried out by repeating the potential at a scan rate of 100 mV s<sup>-1</sup> for 1000 cycles. All current densities are the ratios of currents and geometric areas of working electrodes. The ECSA was elucidated by measuring double layer capacitance (C<sub>dl</sub>) of cyclic voltammetry (CV) at non-Faradaic potentials (0.115-0.215 V in 0.5 M H<sub>2</sub>SO<sub>4</sub> vs RHE and scan rates from 2 to 12 mV s<sup>-1</sup>, 0.52-0.62V in 1.0 M KOH versus RHE and scan rates from 6 to 36 mV s<sup>-1</sup>, respectively) recorded at different scan rates. Electrochemical Impedance Spectroscopy (EIS) measurement was measured in the frequency range of 0.01Hz-100 kHz.

## II Supplementary Structural Section

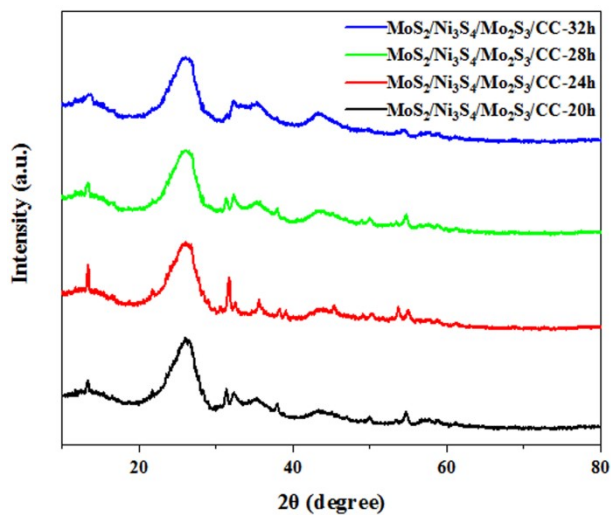


**Fig.S2** PXRD of MoS<sub>2</sub>/Ni<sub>3</sub>S<sub>4</sub>/Mo<sub>2</sub>S<sub>3</sub>/CC-xh (x = 20, 24, 28 and 32 h)

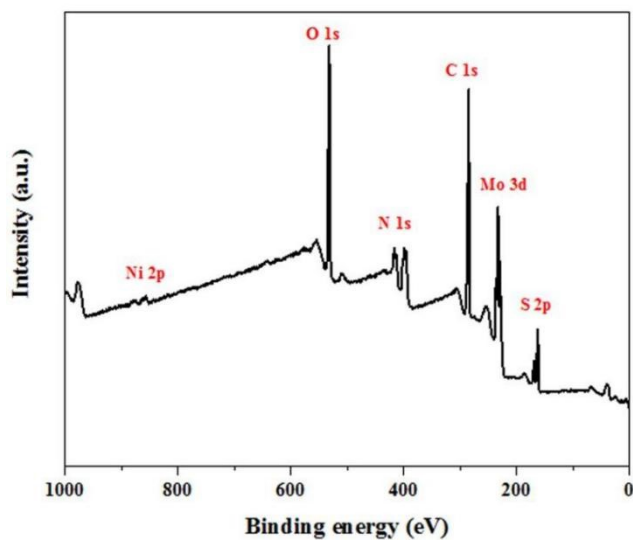


**Fig.S3** XPS spectrum of MoS<sub>2</sub>/Ni<sub>3</sub>S<sub>4</sub>/Mo<sub>2</sub>S<sub>3</sub>/CC-24h

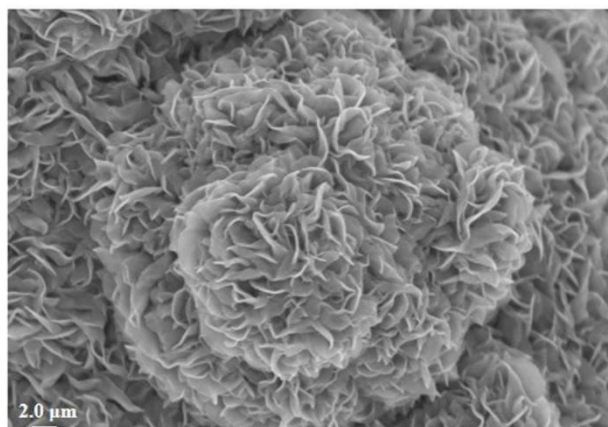


**Fig.S4** SEM image of MoS<sub>2</sub> and Ni<sub>3</sub>S<sub>4</sub> nanosheets

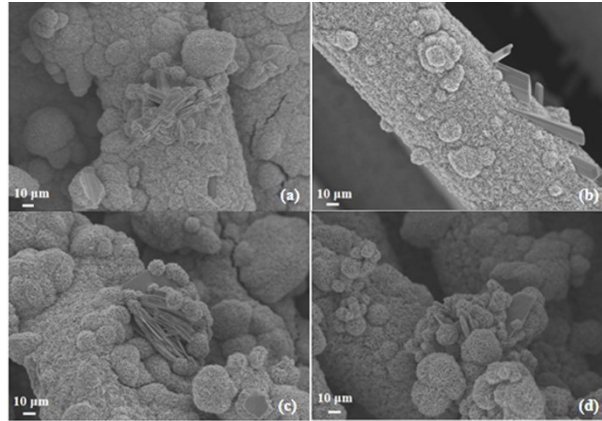


**Fig.S5** SEM images of MoS<sub>2</sub>/Ni<sub>3</sub>S<sub>4</sub>/Mo<sub>2</sub>S<sub>3</sub>/CC-xh (a) 20h; (b) 24h; (c) 28h and (d) 32h

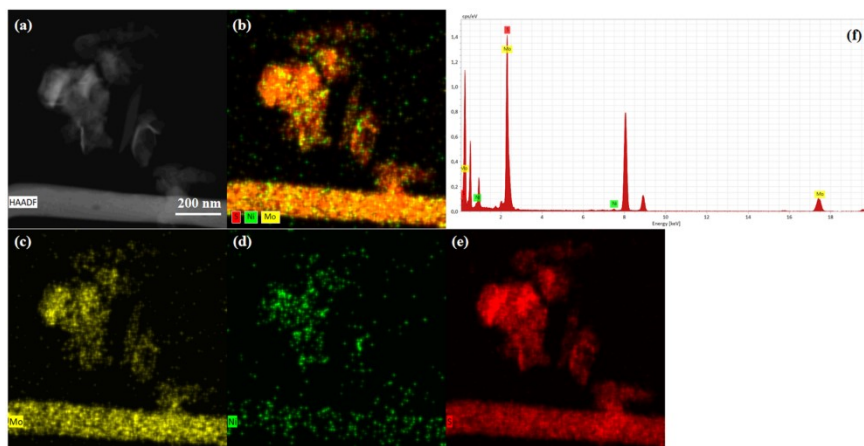


**Fig.S6** (a-e)The EDS mapping; (f)the EDS microanalysis of MoS<sub>2</sub>/Ni<sub>3</sub>S<sub>4</sub>/Mo<sub>2</sub>S<sub>3</sub>/CC-24h

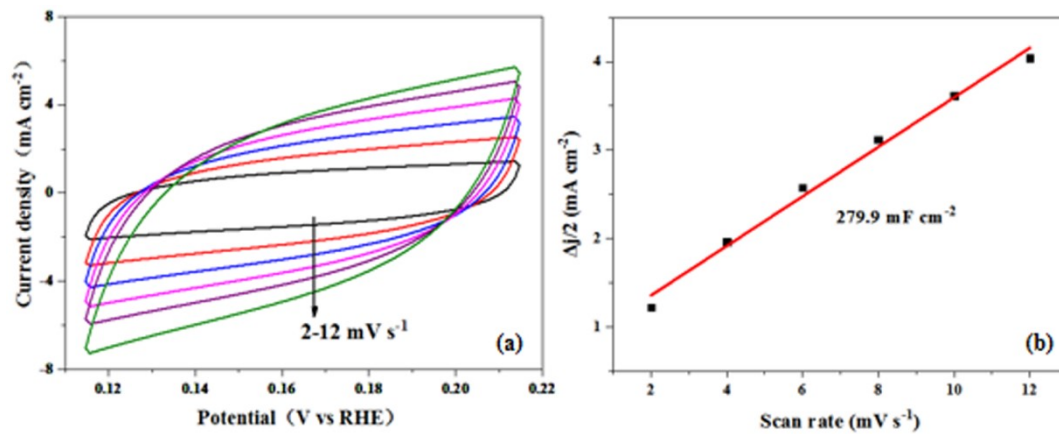


**Fig.S7** (a) CV curves between the potential of 0.115-0.215 V; (b) C<sub>dl</sub> according to the CV curves for MoS<sub>2</sub>/Ni<sub>3</sub>S<sub>4</sub>/Mo<sub>2</sub>S<sub>3</sub>/CC-20h in 0.5 M H<sub>2</sub>SO<sub>4</sub> solution.

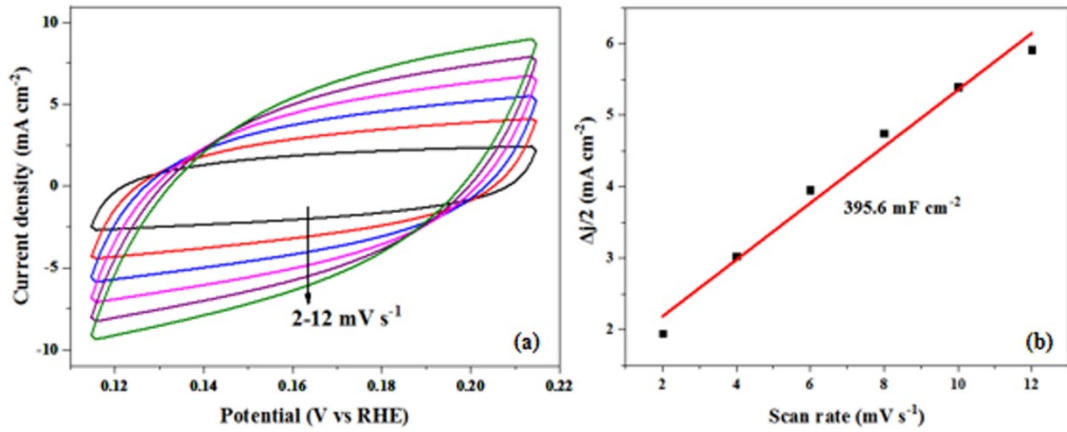


**Fig.S8** (a) CV curves between the potential of 0.115-0.215 V; (b)  $C_{dl}$  according to the CV curves for MoS<sub>2</sub>/Ni<sub>3</sub>S<sub>4</sub>/Mo<sub>2</sub>S<sub>3</sub>/CC-24h in 0.5 M H<sub>2</sub>SO<sub>4</sub> solution.

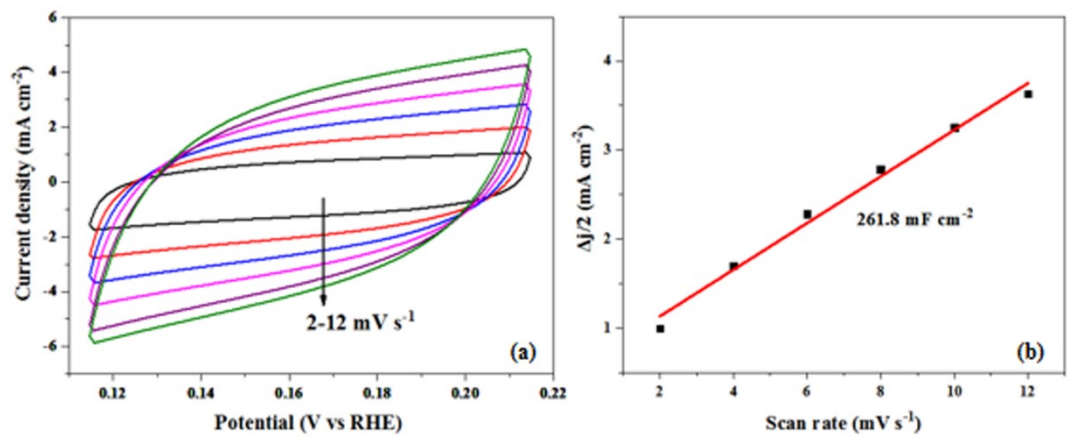


**Fig.S9** (a) CV curves between the potential of 0.115-0.215 V; (b)  $C_{dl}$  according to the CV curves for MoS<sub>2</sub>/Ni<sub>3</sub>S<sub>4</sub>/Mo<sub>2</sub>S<sub>3</sub>/CC-28h in 0.5 M H<sub>2</sub>SO<sub>4</sub> solution.

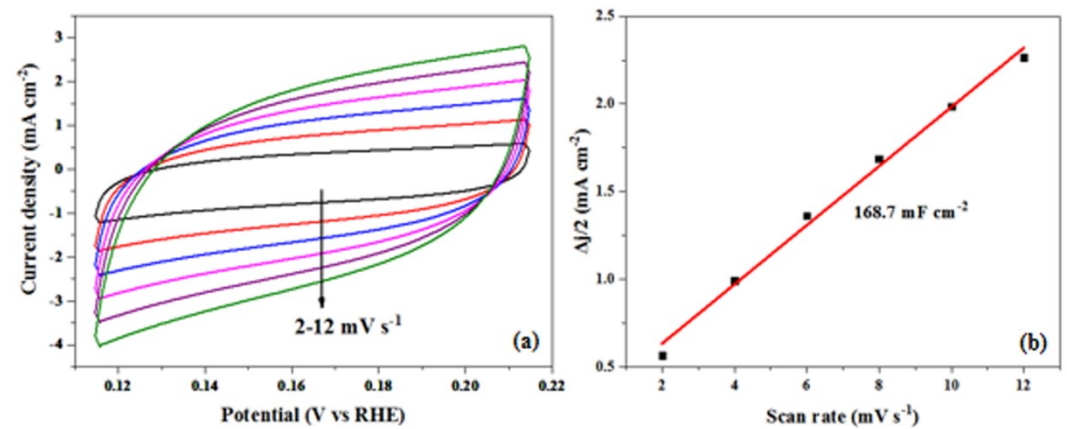


**Fig.S10** (a) CV curves between the potential of 0.115-0.215 V; (b)  $C_{dl}$  according to the CV curves for MoS<sub>2</sub>/Ni<sub>3</sub>S<sub>4</sub>/Mo<sub>2</sub>S<sub>3</sub>/CC-32h in 0.5 M H<sub>2</sub>SO<sub>4</sub> solution.

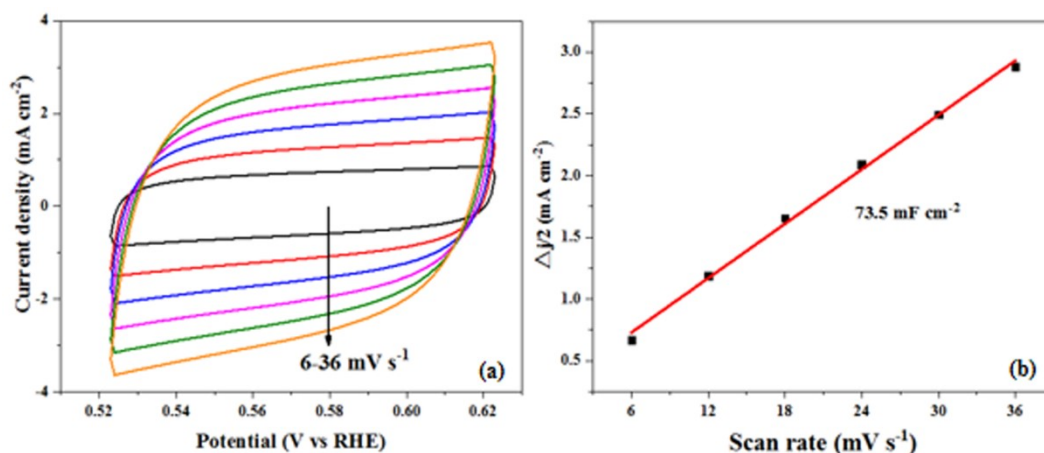


**Fig.S11** (a) CV curves between the potential of 0.52-0.62 V; (b)  $C_{dl}$  according to the CV curves for MoS<sub>2</sub>/Ni<sub>3</sub>S<sub>4</sub>/Mo<sub>2</sub>S<sub>3</sub>/CC-20h in 1 M KOH solution.

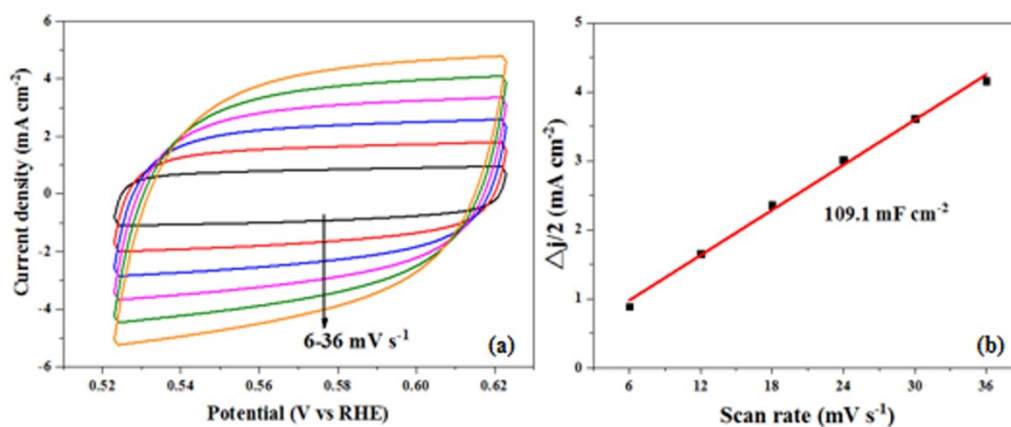


**Fig.S12** (a) CV curves between the potential of 0.52-0.62 V; (b)  $C_{dl}$  according to the CV curves for MoS<sub>2</sub>/Ni<sub>3</sub>S<sub>4</sub>/Mo<sub>2</sub>S<sub>3</sub>/CC-24h in 1 M KOH solution.

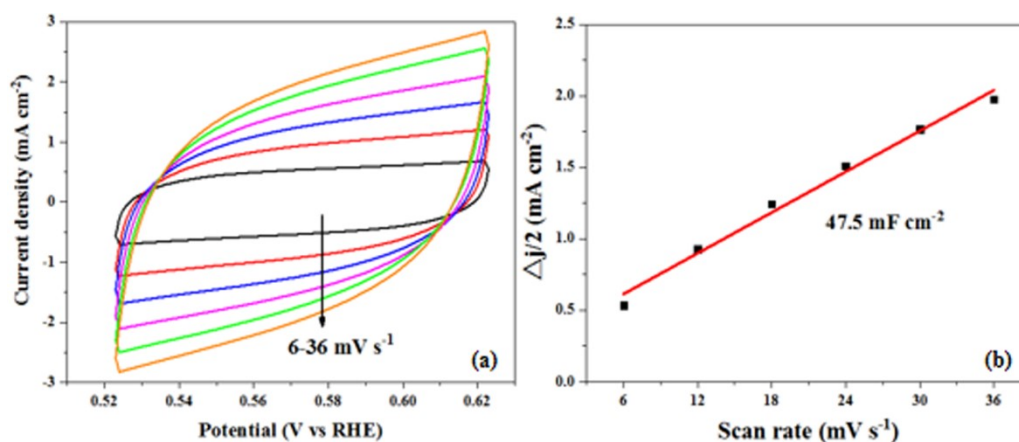


**Fig.S13** (a) CV curves between the potential of 0.52-0.62 V; (b)  $C_{dl}$  according to the CV curves for MoS<sub>2</sub>/Ni<sub>3</sub>S<sub>4</sub>/Mo<sub>2</sub>S<sub>3</sub>/CC-28h in 1 M KOH solution.



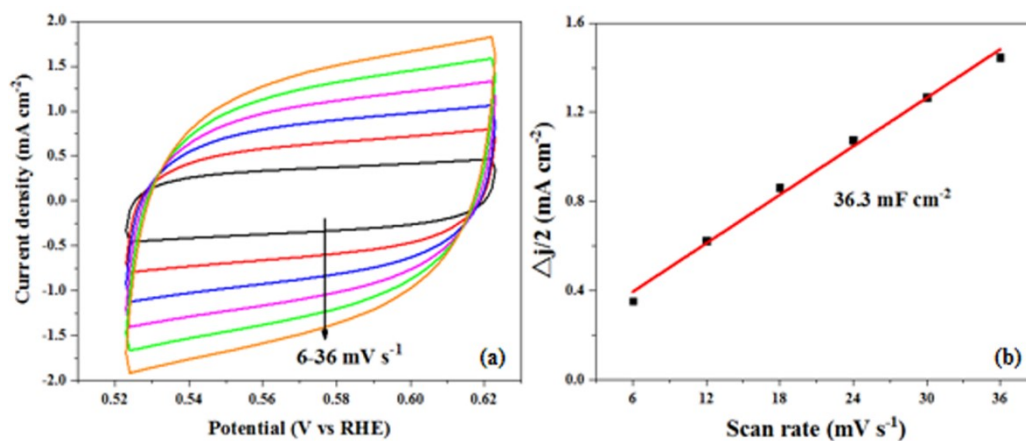


**Fig.S14** (a) CV curves between the potential of 0.52-0.62 V; (b)  $C_{dl}$  according to the CV curves for MoS<sub>2</sub>/Ni<sub>3</sub>S<sub>4</sub>/Mo<sub>2</sub>S<sub>3</sub>/CC-32h in 1 M KOH solution.

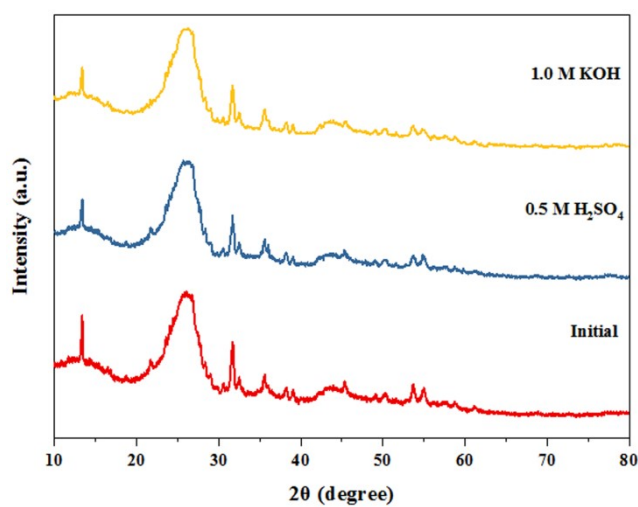


**Fig.S15** PXRD pattern of MoS<sub>2</sub>/Ni<sub>3</sub>S<sub>4</sub>/Mo<sub>2</sub>S<sub>3</sub>/CC-24h after various electrochemistry measurements in 0.5 M H<sub>2</sub>SO<sub>4</sub> and 1.0 M KOH electrolytes.

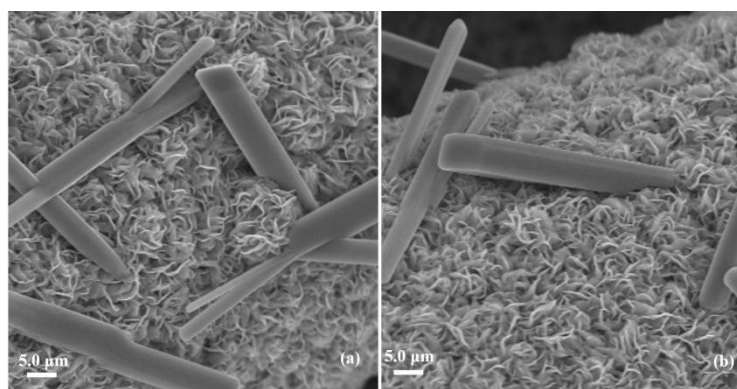


**Fig.S16** The SEM images of MoS<sub>2</sub>/Ni<sub>3</sub>S<sub>4</sub>/Mo<sub>2</sub>S<sub>3</sub>/CC-24h after various electrochemical tests in (a) 0.5 M H<sub>2</sub>SO<sub>4</sub> and (b) 1.0 M KOH solution.

**Table S1.** Comparison of HER performance of similar composite catalysts in 0.5 M H<sub>2</sub>SO<sub>4</sub> and 1.0 M KOH electrolytes.

Catalyst	Counter electrode	Electrolyte	$\eta_{10}$ (mV vs. RHE)	Tafel slops (mV dec <sup>-1</sup> )	References
MoS <sub>2x</sub> Se <sub>2(1-x)</sub>	graphite rod	0.5 M H <sub>2</sub> SO <sub>4</sub>	188	43	2
Se-MoS <sub>2</sub> -NF	graphite rod	0.5 M H <sub>2</sub> SO <sub>4</sub>	132	75	3
S-vacancy MoS <sub>2</sub>	Pt	0.5 M H <sub>2</sub> SO <sub>4</sub>	131	48	4
MoS <sub>2</sub> @CoS <sub>2</sub>	graphite rod	0.5 M H <sub>2</sub> SO <sub>4</sub>	96	60	5
Co-1T-MoS <sub>2</sub>	graphite rod	0.5 M H <sub>2</sub> SO <sub>4</sub>	84	47	6
MoS <sub>2</sub> /CoS <sub>2</sub> -10	graphite rod	0.5 M H <sub>2</sub> SO <sub>4</sub>	69	62	7
Rh-MoS <sub>2</sub>	graphite rod	0.5M H <sub>2</sub> SO <sub>4</sub>	67	54	8
Co-MoS <sub>2</sub>	graphite rod	0.5M H <sub>2</sub> SO <sub>4</sub>	56	32	9
NiO@1T-MoS <sub>2</sub>	graphite rod	0.5M H <sub>2</sub> SO <sub>4</sub>	46	52	10
MoS <sub>2</sub> /Ni <sub>3</sub> S <sub>4</sub> /Mo <sub>2</sub> S <sub>3</sub> /CC	graphite rod	0.5 M H <sub>2</sub> SO <sub>4</sub>	38	84	This work
1T-2H MoS <sub>2</sub>	graphite rod	1.0 M KOH	290	65	11
NiS <sub>2</sub> /MoS <sub>2</sub>	Pt wire	1.0 M KOH	148	70	12
Ni <sub>3</sub> S <sub>4</sub> -MoS <sub>2</sub>	Pt	1.0 M KOH	116	81	13
MoS <sub>2</sub> /Ni <sub>3</sub> S <sub>2</sub>	Pt rod	1.0 M KOH	110	83	14
MoS <sub>2</sub> -Ni <sub>3</sub> S <sub>2</sub> (UR-2)/NF	graphite rod	1.0 M KOH	98	74.8	15
MoS <sub>2</sub> -Ni <sub>3</sub> S <sub>2</sub> HNRs/NF	graphite rod	1.0 M KOH	98	61	16
Ni <sub>3</sub> S <sub>2</sub> @MoS <sub>2</sub> /FeOOH	graphite rod	1.0 M KOH	95	85	17
MoS <sub>2</sub> /NiS	graphite rod	1.0 M KOH	92	113	18
MoS <sub>2</sub> /NiS/MoO <sub>3</sub>	graphite rod	1.0 M KOH	91	55	19
MoS <sub>2</sub> /Ni <sub>3</sub> S <sub>4</sub> /Mo <sub>2</sub> S <sub>3</sub> /CC	graphite rod	1.0 M KOH	51	83	This work

### Supplementary References

- 1 K.Nomiya, T.Takahashi, T.Shirai and M.Miwa, *Polyhedron*,1987, **6**, 213–218.
- 2 Y. C. Huang, Y. H. Sun, X. L. Zheng, T. Aoki, B. Pattengale, J. E. Huang, X. He, W. Bian, S. Younan, N. Williams, J. Hu, J. Q. Ge, N. Pu, X. X. Yan, X. Q. Pan, L. J. Zhang, Y. G. Wei and J. Gu, *Nature Commun.*, 2019, **10**, 982-993.
- 3 C. L. Zhen, B. Zhang, Y. H. Zhou, Y. C. Du and P. Xu,*Inorg. Chem. Front.*, 2018, **5**, 1386-1390.

- 4 B. Ouyang, S. Feng, J. Huo and S. Y. Wang, *Green Energy Environ.*, 2017, **2**, 134-141.
- 5 Z. L. Zheng, L. Yu, M. Gao, X. Y. Chen, W. Zhou, C. Ma, L. H. Wu, J. F. Zhu, X. Y. Meng, J. T. Hu, Y. C. Tu, S. S. Wu, J. Mao, Z. Q. Tian and D. H. Deng, *Nature Commun.*, 2020, **11**, 3315.
- 6 W. Qiao, W. Xu, X. Y. Xu, L. Q. Wu, S. M. Yan and D. H. Wang, *ACS Appl. Energy. Mater.*, 2020, **3**, 2315–2322.
- 7 S. He, H. F. Du, K. Wang, Q. C. Liu, J. M. Sun, Y. H. Liu, Z. Z. Du, L. H. Xie, W. Ai and W. Huang, *Chem. Commun.*, 2020, **56**, 5548-5551.
- 8 Q. Jin, N. Liu, C. N. Dai, R. N. Xu, B. Wu, G. Q. Yu, B. H. Chen and Y. Z. Du, *Adv. Energy. Mater.*, 2020, **10**, 2000291.
- 9 X. Wang, Y. W. Zhang, H. N. Si, Q. H. Zhang, J. Wu, L. Gao, X. F. Wei, Y. Sun, Q. L. Liao, Z. Zhang, K. Ammarah, L. Gu, Z. Kang and Y. Zhang, *J. Am. Chem. Soc.*, 2020, **142**, 4298-4308.
- 10 X. Y. Meng, C. Ma, L. Z. Jiang, R. Si, X. G. Meng, Y. C. Tu, L. Yu, X. H. Bao and D. H. Deng, *Angew. Chem. Int. Ed*, 2020, **59**, 10502-10507.
- 11 T. C. An, Y. Wang, J. Tang, W. Wei, X. Q. Cui, A. M. Alenizi, L. J. Zhang and G. F. Zheng, *J. Mater. Chem. A*, 2016, **4**, 13439-13443.
- 12 Y. Yang, K. Zhang, H. Lin, X. Li, H.C. Chan, L. Yang and Q. Gao, *ACS Catal.*, 2017, **7**, 2357-2366.
- 13 M. Zheng, K. Guo, W. J. Jiang, T. Tang, X. Wang, P. Zhou, J. Du, Y. Zhao, C. Xu and J. S. Hu, *Appl. Catal. B*, 2019, **244**, 1004-1012.
- 14 J. Zhang, T. Wang, D. Pohl, B. Rellinghaus, R. Dong, S. Liu, X. Zhuang and X. Feng, *Angew. Chem. Int. Ed*, 2016, **55**, 6702-6707.
- 15 C. Q. Wang, B. Tian, M. Wu and J. H. Wang, *ACS Appl. Mater. Inter.*, 2017, **9**, 7084-7090.
- 16 J. M. Ge, J. X. Jin, Y. M. Cao, M. H. Jiang, F. Z. Zhang, H. L. Guo and X. D. Lei, *RSC Adv.*, 2021, **11**, 19630-19638.
- 17 S. Wang, D. Zhang, B. Li, C. Zhang, Z. G. Du, H. M. Yin, X. F. Bi and S. H. Yang, *Adv. Energy Mater.*, 2018, **8**, 1801345.
- 18 Z. J. Zhai, C. Li, L. Zhang, H. C. Wu, L. Zhang, N. Tang, W. Wang and J. L. Gong, *J. Mater. Chem. A*, 2018, **6**, 9833-9838.

19 Y. Q. Liu, Y. Yu, Z. C. Mu, Y. H. Wang, U. Ali, S. Y. Jing and S. X. Xing, *Inorg. Chem. Front.*, 2020, 7, 3588-3597.

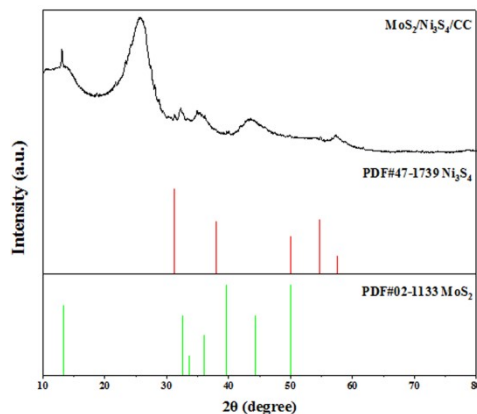


Fig.S17 PXR D patterns of MoS<sub>2</sub>/Ni<sub>3</sub>S<sub>4</sub>/CC, Ni<sub>3</sub>S<sub>4</sub> and MoS<sub>2</sub>.

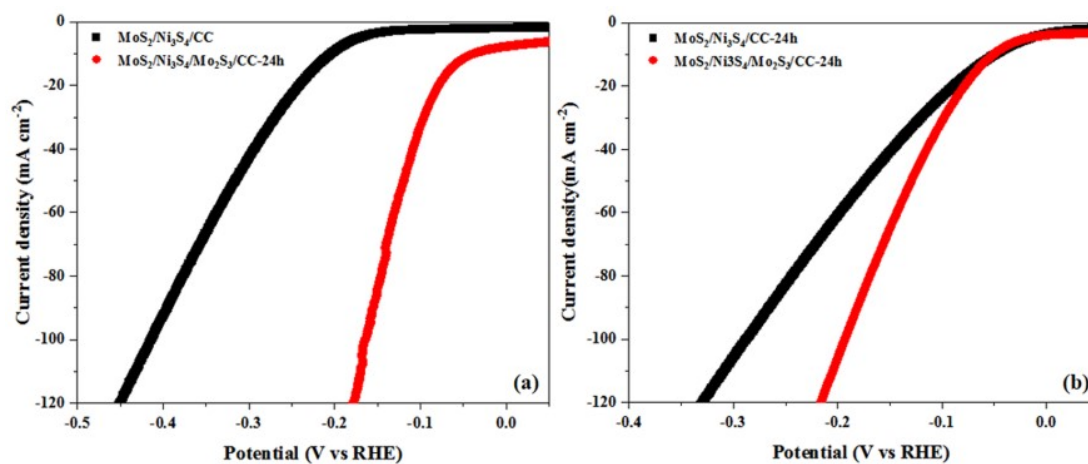


Fig.S18 The polarization curves of MoS<sub>2</sub>/Ni<sub>3</sub>S<sub>4</sub>/CC and MoS<sub>2</sub>/Ni<sub>3</sub>S<sub>4</sub>/Mo<sub>2</sub>S<sub>3</sub>/CC-24h (a) in 0.5 M H<sub>2</sub>SO<sub>4</sub> electrolyte and (b) 1.0 M KOH electrolyte.

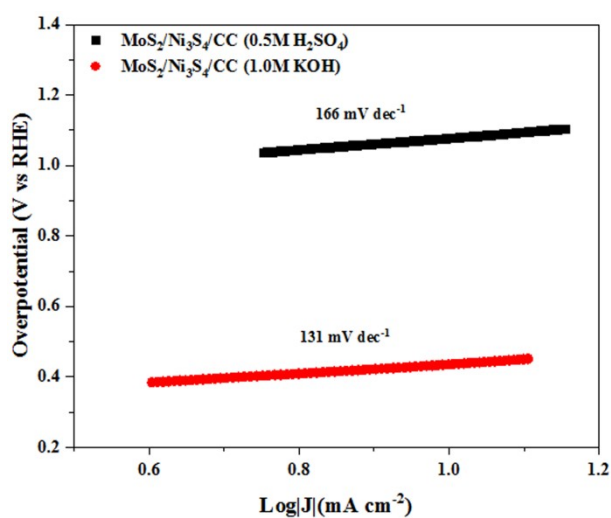
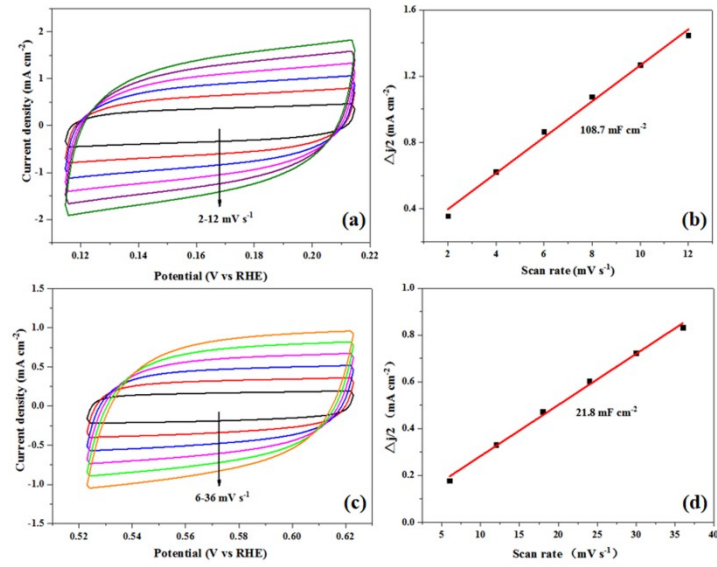


Fig.S19 The Tafel plots of MoS<sub>2</sub>/Ni<sub>3</sub>S<sub>4</sub>/CC in 0.5 M H<sub>2</sub>SO<sub>4</sub> and 1.0 M KOH electrolytes.



**Fig.S20** (a) CV curves between the potential of 0.115- 0.215 V; (b)  $C_{dl}$  according to the CV curves for MoS<sub>2</sub>/Ni<sub>3</sub>S<sub>4</sub>/CC in 0.5 M H<sub>2</sub>SO<sub>4</sub> solution; (c) CV curves between the potential of 0.52- 0.62 V; (d)  $C_{dl}$  according to the CV curves for MoS<sub>2</sub>/Ni<sub>3</sub>S<sub>4</sub>/CC in 1 M KOH solution.